

Cruise Report

S-244 Oceans & Climate

Scientific Data Collected Aboard
SSV Robert C. Seamans

Honolulu, Hawaii, USA – Papeete, Tahiti, French Polynesia
15 November 2012 – 23 December 2012



Sea Education Association
Woods Hole, Massachusetts

This document should be cited as:

Meyer, A.W. 2013. Final report for S.E.A. Cruise S244. Sea Education Association, Woods Hole, MA 02543. www.sea.edu.

To obtain unpublished data, contact the Chief Scientist or SEA data archivist:

Data Archivist
Sea Education Association
PO Box 6
Woods Hole, MA 02543
Phone: 508-540-3954
Fax: 508-457-4673
E-mail: data-archives@sea.edu
Web: www.sea.edu

Table of Contents

Ship's Company	4
Introduction	5
Table 1. Student Research Projects, S-244	6
Data Description	7
Figure 1. S-244 Cruise Track	7
Table 2. Oceanographic Sampling Stations	8
Table 3. Surface Sampling Station Data	10
Figure 2. Surface Current Direction and Magnitude	12
Figure 3. East-west Current Velocity Component	12
Figure 4. Surface Temperature and Salinity	13
Figure 5. Cross Section of Temperature and Salinity	14
Figure 6. Cross Section of Oxygen and Fluorescence	15
Table 4. Hydrocast Bottle Data	16
Table 5. Neuston Net Data	22
Table 6. Meter Net Data	24
Table 7. Tucker Trawl Data	25
Student Research Abstracts	26

Ship's Company

SSV *Robert C. Seamans*, Cruise S-244

Nautical Staff

Pamela Coughlin	Captain
Ryan Shamburger	Chief Mate
Will McLean	Second Mate
Ashley Meyer	Third Mate
Seth Murray	Engineer
Mickey Cavacas	Assistant Engineer
Abby Cazeault	Steward
Matt Ecklund	Deckhand
Tristan Feldman	Deckhand
Melissa Ibarra	Deckhand

Scientific Staff

Audrey Meyer	Chief Scientist
Carla Scocchi	First Assistant Scientist
Laura Hansen	Second Assistant Scientist
Juliana Miller	Third Assistant Scientist

Students

Mindy Alexander	Cornell University
Samantha Allen	University of Denver
Darcy E. Balcarce	SUNY College of Environmental Science & Forestry
Katie Blacketer	Oregon State University
Ariel Christensen	College of Charleston
Simona Clausnitzer	Bryn Mawr College
Michela Cupo	Roger Williams University
Ivan Duong	Carleton College
Jennifer Fardy	University of Massachusetts, Amherst
Jack Fields	Cornell University
Madison Halloran	Carleton College
Trevor Kauffman	University of Pennsylvania
Hayli Kinney	Amherst College
Rebecca Lehman	Colorado College
Brendan O'Flaherty	Lawrence University
Ashley O'Neill	Vassar College
Souha Ouni	Barnard College
Shenandoah Raycroft	College of William & Mary
Mary Kathryn Rutz	Cornell University
Marta Trodahl	University of Stavanger
Leona Waller	Colorado College

Introduction

This cruise report provides a summary of scientific activities aboard the SSV *Robert C. Seamans* during cruise S-244 (15 November – 23 December 2012). This was the sea component of an oceanography-focused 'Oceans & Climate' SEA Semester program, during which undergraduate science majors examined how the global ocean functions in the climate system. Research was conducted throughout our 2900nm transect from Hawaii to Tahiti, as we sailed from the southern part of the North Pacific Subtropical Gyre, across the equatorial region with its complex and dynamic current systems, to the northern part of the South Pacific Subtropical Gyre. While onboard, the students served as full, working members of the scientific team and sailing crew, deploying oceanographic sampling equipment, managing shipboard operations, and conducting independent project research related to climate change. They completed two academic courses (*Oceanographic Field Methods* and *Directed Oceanographic Research*), earning upper-division credit at Boston University for subsequent transfer to their home institutions. Extensive oceanographic sampling was conducted for both student research projects (Table 1) and the ongoing SEA research program. Students examined the diverse physical, chemical, biological, and environmental oceanographic characteristics in accordance with their written proposals prepared onshore before sailing, and presented their results in a final poster session and papers (available upon request from SEA).

The brief summary of data contained in this report is not intended to represent final data interpretation and should not be excerpted or cited without written permission from SEA.

Audrey W. Meyer
Chief Scientist, S-244

Table 1. Student research projects, S-244.

Title	Student Investigator(s)
Are Barrier Layers Indicative of Imminent ENSO Events?	Michela Cupo Shenandoah Raycroft
Pacific Salp Gut Chlorophyll Content vs. Salp Size, Environmental Chlorophyll-a Concentration, and Salp Density	Jack Fields
Effects of El Nino Southern Oscillation on the Equatorial Undercurrent Heat Transport	Souha Ouni
Measuring Skipjack Tuna Habitat in the Central Equatorial Pacific	Trevor Kauffman
Cyanobacteria Abundances Along an Equatorial Pacific Cruise Track	Ariel Christensen Samantha Allen
Dimethylsulfoniopropionate (DMSP) Potential Production in the Equatorial Pacific Biogeochemical Sulfur Cycle: A Measure of Phytoplankton Abundances	Darcy Balcarce Simona Clausnitzer
Effects of Predator Presence, Biodiversity, and Nighttime Light Intensity on Diel Vertical Migration in the Equatorial Pacific	Ashley O'Neill Brendan O'Flaherty
Phytoplankton Size and Total Primary Production in Four Distinct Oceanic Environments	Ivan Duong Hayli Kinney Rebecca Lehman
Patterns of <i>Myctophid</i> Distribution and Diversity in the Central Pacific	Katie Blacketer
Heat Transport Along a Meridional Transect of the Pacific Equatorial Region	Marta Trodahl Jennifer Fardy
Pteropod Distribution in the Equatorial Pacific: Implications of Acidifying Waters	Mindy Alexander Mary Rutz
Going With the Flow: An Analysis of Surface Water Masses in the Equatorial Pacific	Madison Halloran Leona Waller

Data Description

This section provides a record of data collected aboard the SSV *Robert C. Seamans* cruise S-244 (US State Department Cruise F2012-053) from Honolulu, Hawaii to Papeete, Tahiti, French Polynesia (Figure 1).

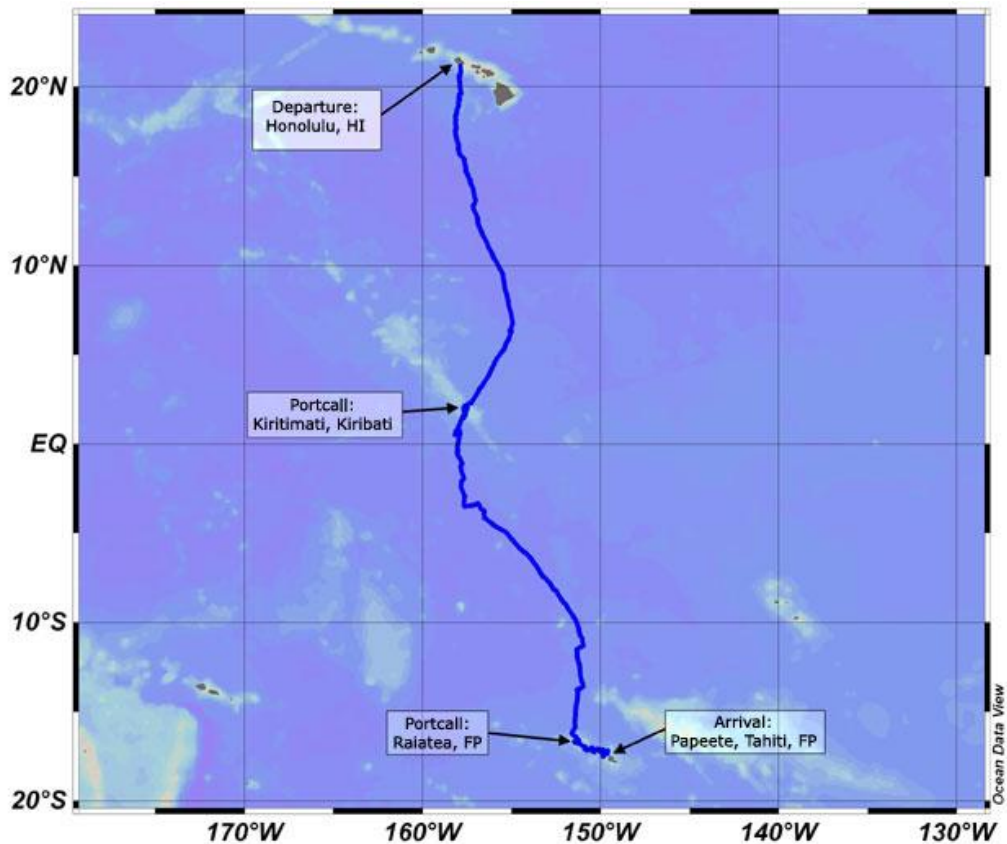


Figure 1. Hourly positions along the S-244 cruise track.

During the 6-week voyage, we sampled at 45 discrete oceanographic stations (Table 2). Chemical analyses were made of 45 surface water samples, 40 of which occurred coincident with hydrocast and biological sampling (neuston net, meter net, and Tucker Trawl) stations (Table 3). Additionally, we continuously sampled water depth and sub-bottom profiles (CHIRP system), upper ocean currents (ADCP, Figures 2 and 3), and sea surface temperature, salinity, colored dissolved organic matter (CDOM), and transmittance (seawater flow-through system, Figure 4 – temperature, salinity). Discrete CTD measurements of vertical temperature and salinity profiles are presented in Figure 5. Additional instrumentation on the CTDs allowed for profiling of dissolved oxygen, fluorescence, transmittance, photosynthetically active radiation (PAR) and CDOM (Figure 6). Summaries of sea surface and water column chemical and biological properties are found in Tables 4-7. Lengthy CTD, CHIRP, ADCP and flow-through data are not fully presented here. All unpublished data can be made available by arrangement with the SEA data archivist (contact information, p. 2).

Table 2. Oceanographic sampling stations. **X** indicates type of station. (NT = Neuston Tow, MN = Meter Net, TT = Tucker Trawl, PN = Phytoplankton Net, HC = Hydrocast with CTD, CTD = Free CTD, RBR = Minilogger depth and temperature recorder, SS = Surface Station. See additional footnotes at bottom of table, continued on next page.

Station	Date	Time	Latitude	Longitude	General Locale ¹	NT	MN ²	TT	PN	HC	CTD	RBR	SS ³
S244-001	17-Nov-12	2244	20°40.7' N	157°55.4' W	Off Hawaii	X							SS-001
S244-002	18-Nov-12	1102	19°45.8' N	157°52.1' W	NPSG				X	X			#13
S244-003	18-Nov-12	2220	19°16.5' N	157°57.2' W	NPSG	X				X			#13
S244-004	19-Nov-12	1102	18°25.7' N	158°8.3' W	NPSG					X			#13
S244-005	19-Nov-12	2110	17°41.8' N	157°53.0' W	NPSG			X		X			#13
S244-006	20-Nov-12	1055	16°38.0' N	158°0.3' W	NPSG			X					
S244-007	20-Nov-12	2119	15°56.0' N	157°39.6' W	NPSG	X			X	X			#13
S244-008	21-Nov-12	0915	15°6.7' N	157°28.0' W	NPSG					X			#13
S244-009	21-Nov-12	2100	14°13.1' N	157°8.3' W	NEC	X			X	X			#13
S244-010	22-Nov-12	0942	13°23.8' N	157°8.7' W	NEC		X(A/B)			X			#13
S244-011	22-Nov-12	2115	12°34.0' N	156°54.3' W	NEC	X	X(A/B)			X			#13
S244-012	23-Nov-12	0900	11°43.6' N	156°38.3' W	NEC/ITCZ					X			#13
S244-013	23-Nov-12	2105	10°34.6' N	156°3.7' W	ITCZ	X			X	X			#13
S244-014	24-Nov-12	0916	9°29.3' N	155°29.4' W	ITCZ					X			#13
S244-015	24-Nov-12	2108	8°2.7' N	155°13.1' W	NECC	X			X	X			#13
S244-016	25-Nov-12	0914	6°45.7' N	154°57.8' W	NECC		X(A/B)			X		X	#13
S244-017	25-Nov-12	2100	5°54.7' N	155°9.6' W	NECC	X	X(A/B)		X	X			#13
S244-018	26-Nov-12	0915	5°13.3' N	155°30.5' W	NECC					X			#13
S244-019	26-Nov-12	2122	4°13.8' N	156°6.7' W	NECC	X			X	X			#13
S244-020	27-Nov-12	2118	2°16.8' N	157°19.8' W	N. of Kirimati	X			X	X			#13
S244-021	2-Dec-12	2109	1°35.5' N	157°38.3' W	SEC	X			X	X			#13
S244-022	3-Dec-12	0911	1°33.9' N	157°39.2' W	SEC	X				X			#13
S244-023	3-Dec-12	2150	1°46.5' N	158°2.9' W	SEC	X			X	X			#13
S244-024	4-Dec-12	0853	0°35.2' N	157°53.8' W	SEC/EUC	X							
S244-025	4-Dec-12	2111	0°22.9' S	158°1.7' W	SEC/EUC	X			X	X			#13

Table 2, continued.

Station	Date	Time	Latitude	Longitude	General Locale ¹	NT	MN ²	TT	PN	HC	CTD	RBR	SS ³
S244-026	5-Dec-12	0912	1°9.2' S	157°47.8' W	SEC/EUC	X	X(A/B)			X		X	#13
S244-027	5-Dec-12	2110	1°50.6' S	157°42.5' W	SEC	X	X(A/B)		X	X			#13
S244-028	6-Dec-12	0903	2°55.4' S	157°38.0' W	SEC	X				X			#13
S244-029	6-Dec-12	2109	3°24.8' S	157°12.5' W	SEC	X			X	X			#13
S244-030	7-Dec-12	0905	3°49.0' S	156°32.3' W	SEC	X				X			#13
S244-031	7-Dec-12	2106	4°28.6' S	156°4.6' W	SEC/SPSG	X			X	X			#13
S244-032	8-Dec-12	0907	5°16.6' S	155°3.8' W	SPSG	X	X(A/B)			X			#13
S244-033	8-Dec-12	2152	6°1.8' S	154°19.6' W	SPSG	X	X(A/B)		X	X			#13
S244-034	9-Dec-12	0915	6°38.1' S	153°45.9' W	SPSG	X				X			#13
S244-035	9-Dec-12	2114	7°26.5' S	153°13.7' W	SECC	X			X	X			#13
S244-036	10-Dec-12	0912	8°10.5' S	152°36.9' W	SECC	X	X(A/B)			X			#13
S244-037	10-Dec-12	2110	8°49.8' S	152°7.5' W	SECC	X	X(A/B)			X			#13
S244-038	11-Dec-12	0850	9°40.3' S	151°32.1' W	SECC	X				X			#13
S244-039	11-Dec-12	2128	10°45.9' S	151°8.1' W	SECC	X			X	X			#13
S244-040	12-Dec-12	0905	11°30.1' S	151°20.8' W	SECC/SPSG	X				X			#13
S244-041	12-Dec-12	2108	12°22.9' S	151°12.6' W	SPSG	X			X	X			#13
S244-042	13-Dec-12	0900	13°15.9' S	151°5.2' W	SPSG	X				X			#13
S244-043	13-Dec-12	2116	13°50.8' S	151°19.1' W	SPSG	X			X	X			#13
S244-044	20-Dec-12	0000	17°6.5' S	150°47.6' W	SPSG	X							
S244-045	21-Dec-12	0833	17°13.1' S	150°20.3' W	SPSG						X		

¹ General locale designators: NPSG = North Pacific Subtropical Gyre; NEC = North Equatorial Current; ITCZ = Intertropical Convergence Zone; NECC = North Equatorial Countercurrent; SEC = South Equatorial Current; EUC = Equatorial Undercurrent; SECC = South Equatorial Countercurrent; SPSG = South Pacific Subtropical Gyre.

² Two meter nets were deployed at each MN station, labeled 'Net A' and 'Net B'. In each case, 'Net A' was placed on the deployment wire first, so it was towed at a deeper depth than 'Net B'.

³ Surface station data for hydrocast stations came from water samples collected in lab from flow-through system while carousel was being deployed. These samples are designated as 'Bottle #13'. Blank indicates no surface water sample collected.

Table 3. Surface sampling station data (SS-XXX, XXX-HC). Blanks indicate no sample collected.

Station ¹	Date	Time	Latitude	Longitude	Temp (°C)	Salinity (PSU)	Chl a (ug/l)	PO ₄ (μM)	NO ₃ (μM)
SS-001	17-Nov-12	2246	20°40.7' N	157°55.4' W	26.1	35.23	0.154	0.260	
S244-002-HC #13	18-Nov-12	1102	19°45.8' N	157°52.1' W	26.1	35.26	0.186	0.11	
S244-003-HC #13	18-Nov-12	2220	19°16.5' N	157°57.2' W	26.1	35.25	0.153	0.23	0.17
S244-004-HC #13	19-Nov-12	1102	18°25.7' N	158°8.3' W	26.1	35.26	0.230	0.01	
S244-005-HC #13	19-Nov-12	2110	17°41.8' N	157°53.0' W	26.1	35.26	0.155	0.07	0.25
S244-007-HC #13	20-Nov-12	2119	15°56.0' N	157°39.6' W	26.0	35.01	0.111	0.13	0.12
S244-008-HC #13	21-Nov-12	0915	15°6.7' N	157°28.0' W	26.2	34.85	0.128	0.06	0.14
S244-009-HC #13	21-Nov-12	2100	14°13.1' N	157°8.3' W	26.1	34.60	0.122	0.18	0.17
S244-010-HC #13	22-Nov-12	0942	13°23.8' N	157°8.7' W	26.9	34.50	0.158	0.13	0.05
S244-011-HC #13	22-Nov-12	2115	12°34.1' N	156°54.3' W	27.4	34.50	0.109	0.04	
S244-012-HC #13	23-Nov-12	0900	11°43.6' N	156°38.3' W	27.4	34.30	0.136	0.11	
S244-013-HC #13	23-Nov-12	2105	10°34.6' N	156°3.7' W	27.8	34.31	0.099	0.12	0.09
S244-014-HC #13	24-Nov-12	0916	9°29.3' N	155°29.4' W	27.8	34.21	0.117	0.12	
S244-015-HC #13	24-Nov-12	2108	8°2.7' N	155°13.1' W	28.8	34.40	0.094	0.12	0.33
S244-016-HC #13	25-Nov-12	0914	6°45.7' N	154°57.8' W	29.0	34.41	0.117	0.12	0.19
S244-017-HC #13	25-Nov-12	2100	5°54.7' N	155°9.6' W	29.0	34.82	0.171	0.20	0.52
S244-018-HC #13	26-Nov-12	0915	5°13.3' N	155°30.5' W	29.0	34.90	0.235	0.15	0.91
S244-019-HC #13	26-Nov-12	2122	4°13.8' N	156°6.7' W	27.9	35.09	0.155	1.26	3.03
S244-020-HC #13	27-Nov-12	2118	2°16.8' N	157°19.8' W	28.2	35.22	0.178	0.72	7.12
SS-002	2-Dec-12	1427	1°59.9' N	157°29.7' W	27.5	35.17	0.207	0.59	
SS-003	2-Dec-12	1445	1°58.9' N	157°30.3' W	27.4	35.16	0.239	0.56	
SS-004	2-Dec-12	1503	1°57.5' N	157°31.0' W	27.3	35.18	0.249	0.54	
SS-005	2-Dec-12	1557	1°55.3' N	157°33.5' W	27.7	35.18	0.163	0.54	
S244-021-HC #13	2-Dec-12	2109	1°35.5' N	157°38.3' W	27.9	35.22	0.082	0.52	
S244-022-HC #13	3-Dec-12	0911	1°33.9' N	157°39.2' W	27.9	35.20			
S244-023-HC #13	3-Dec-12	2150	0°46.5' N	158°2.9' W	27.5	35.28	0.207	0.57	9.75
S244-025-HC #13	4-Dec-12	2111	0°22.9' S	158°1.7' W	27.5	35.40	0.193	0.77	11.28
S244-026-HC #13	5-Dec-12	0912	1°9.2' S	157°47.8' W	27.7	35.46	0.348	0.56	12.06
S244-027-HC #13	5-Dec-12	2110	1°50.6' S	157°42.5' W	27.8	35.51	0.216	0.44	13.97
S244-028-HC #13	6-Dec-12	0903	2°55.4' S	157°38.0' W	27.8	35.50	0.202	0.58	13.69

Table 3, continued.

Station	Date	Time	Latitude	Longitude	Temp (°C)	Salinity (PSU)	Chl a (ug/l)	PO ₄ (μM)	NO ₃ (μM)
S244-029-HC #13	6-Dec-12	2109	3°24.8' S	157°12.5' W	28.2	35.70	0.119	0.65	11.30
S244-030-HC #13	7-Dec-12	0905	3°49.0' S	156°32.3' W	28.3	35.65	0.192	0.54	11.25
S244-031-HC #13	7-Dec-12	2106	4°28.6' S	156°4.6' W	28.9	35.66	0.137	0.40	9.60
S244-032-HC #13	8-Dec-12	0907	5°16.6' S	155°3.8' W	28.7	35.62	0.282	0.61	9.60
S244-033-HC #13	8-Dec-12	2152	6°1.8' S	154°19.6' W	28.7	35.64		0.52	9.71
S244-034-HC #13	9-Dec-12	0915	6°38.1' S	153°45.9' W	28.8	35.60	0.187	0.48	8.48
S244-035-HC #13	9-Dec-12	2114	7°26.5' S	153°13.7' W	28.5	35.65		0.12	5.32
S244-036-HC #13	10-Dec-12	0912	8°10.5' S	152°36.9' W	29.3	35.54		0.14	7.96
S244-037-HC #13	10-Dec-12	2110	8°49.8' S	152°7.5' W	29.3	35.54	0.157	0.41	6.37
S244-038-HC #13	11-Dec-12	0850	9°40.3' S	151°32.1' W	29.3	36.40	0.214	0.12	3.56
S244-039-HC #13	11-Dec-12	2128	10°45.9' S	151°8.1' W	29.3	35.48	0.168		1.92
S244-040-HC #13	12-Dec-12	0905	11°30.1' S	151°20.8' W	29.2	35.51	0.248	0.11	
S244-041-HC #13	12-Dec-12	2108	12°22.9' S	151°12.6' W	29.2	35.60	0.137	0.18	1.13
S244-042-HC #13	13-Dec-12	0900	13°15.9' S	151°5.2' W	29.1	35.81	0.149	0.40	0.65
S244-043-HC #13	13-Dec-12	2116	13°50.8' S	151°19.1' W	29.1	35.40	0.127	0.50	0.74

¹ Surface station data for hydrocast stations came from water samples collected in lab from flow-through system while carousel was being deployed. These samples are designated 'Bottle #13' (e.g, S244-043-HC #13).

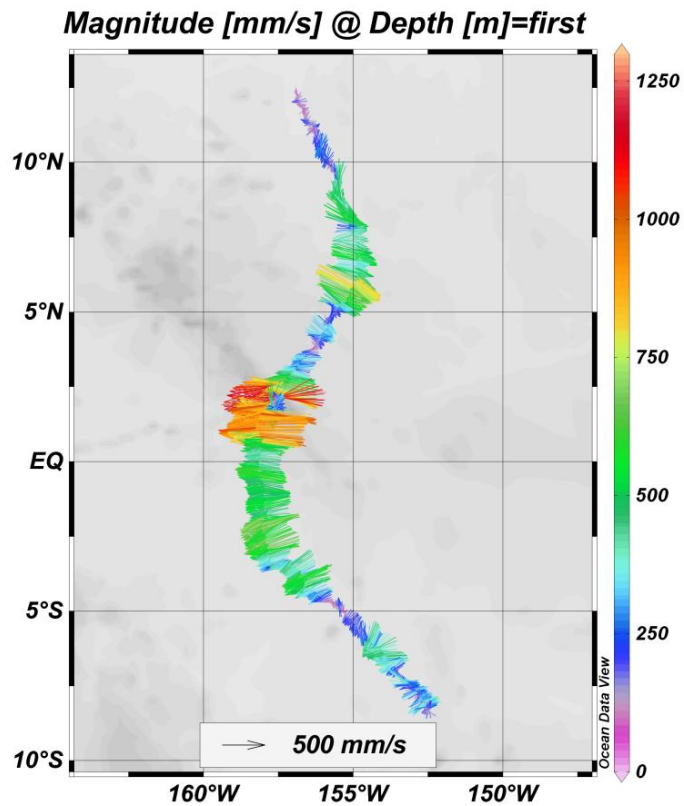


Figure 2. Surface current velocity (direction and magnitude) measured with the ADCP across equatorial current systems traversed during SEA Cruise S-244.

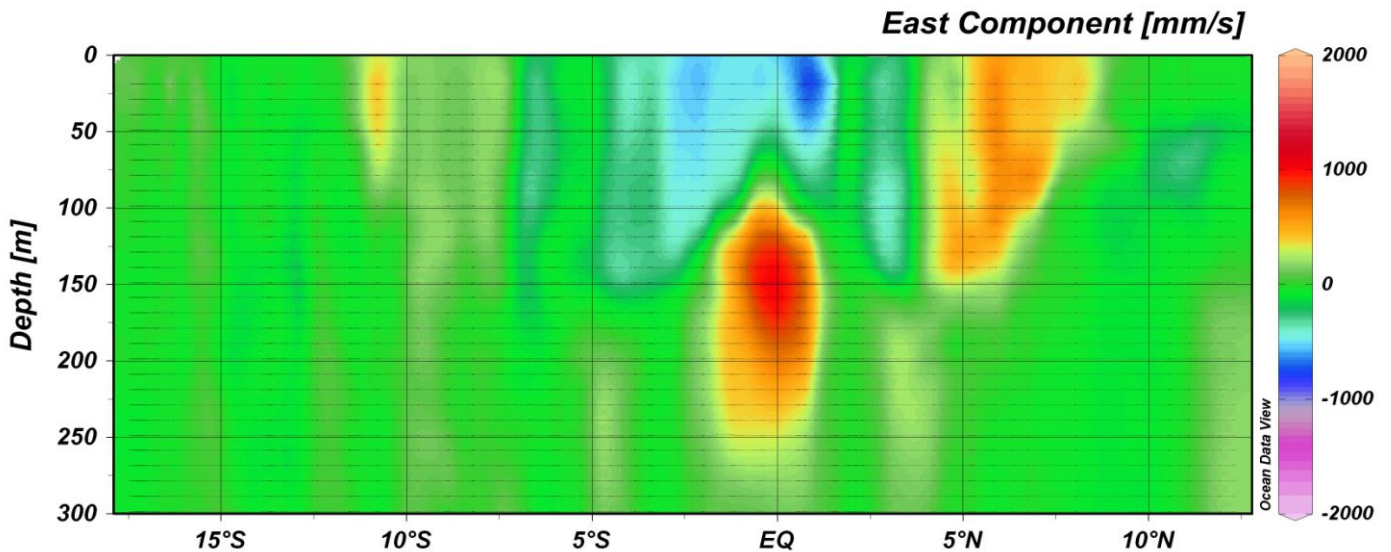
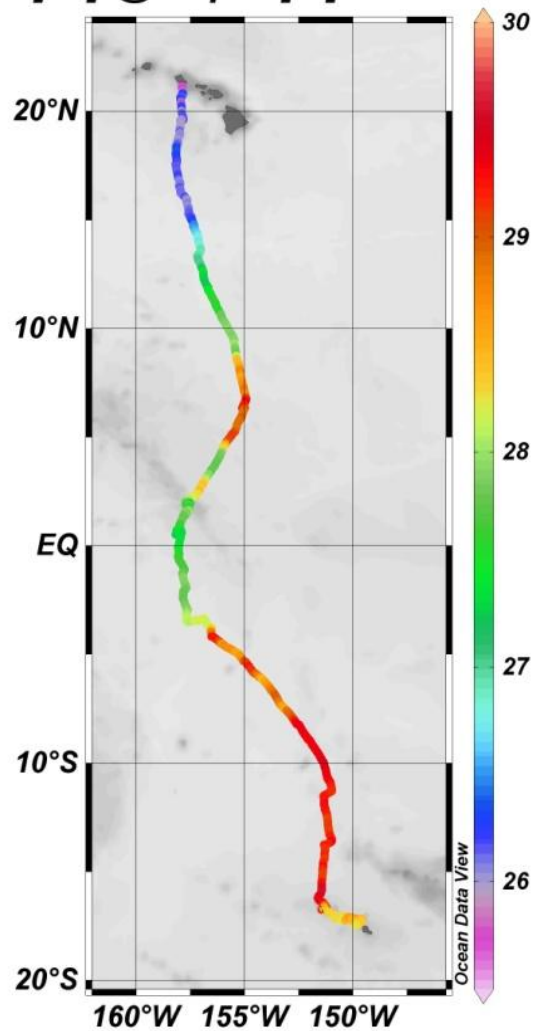


Figure 3. East-west velocity component of currents, in mm/sec, measured along S-244 cruise track. Positive values represent current flow in eastward direction; negative values represent current flow in westward direction.

Temperature [°C] @ Depth [m]=first



Salinity [psu] @ Depth [m]=first

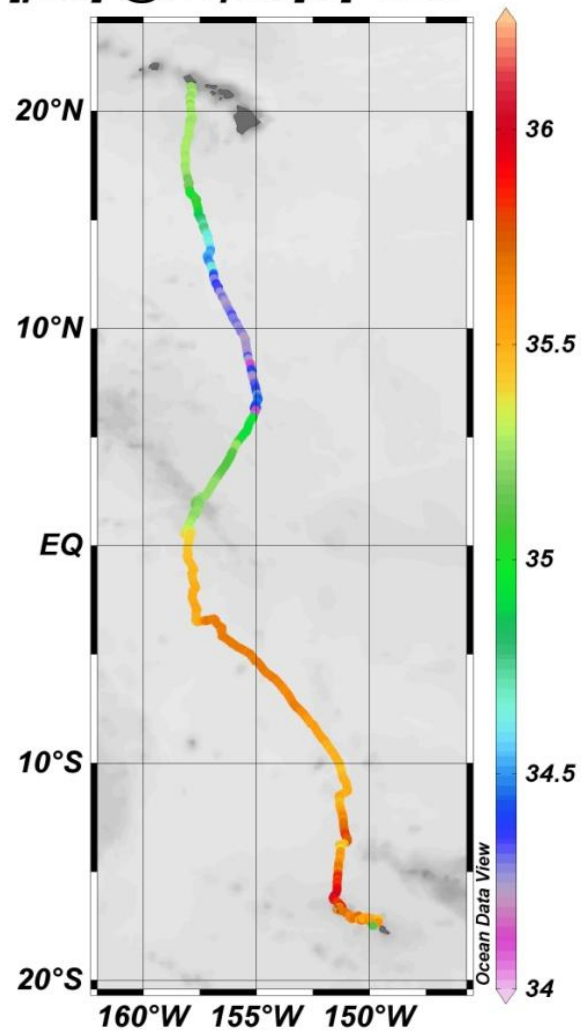


Figure 4. Hourly surface temperature (left figure) and surface salinity measurement (right figure) from the continuous flow-through data logger.

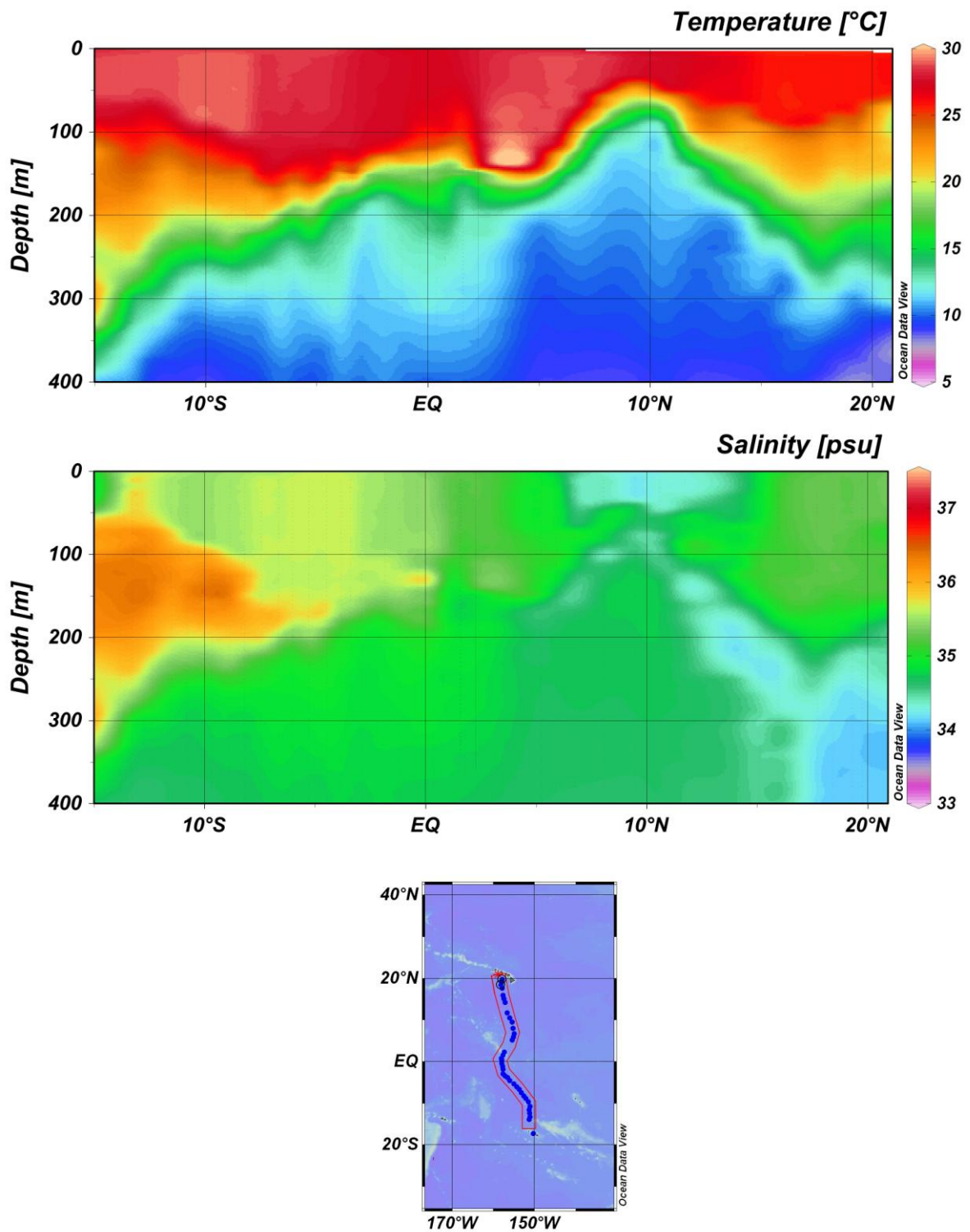


Figure 5. Temperature (top) and salinity (middle) cross sections created from CTD data collected along the entire cruise track. Blue dots on map (bottom) indicate locations of stations included in the section.

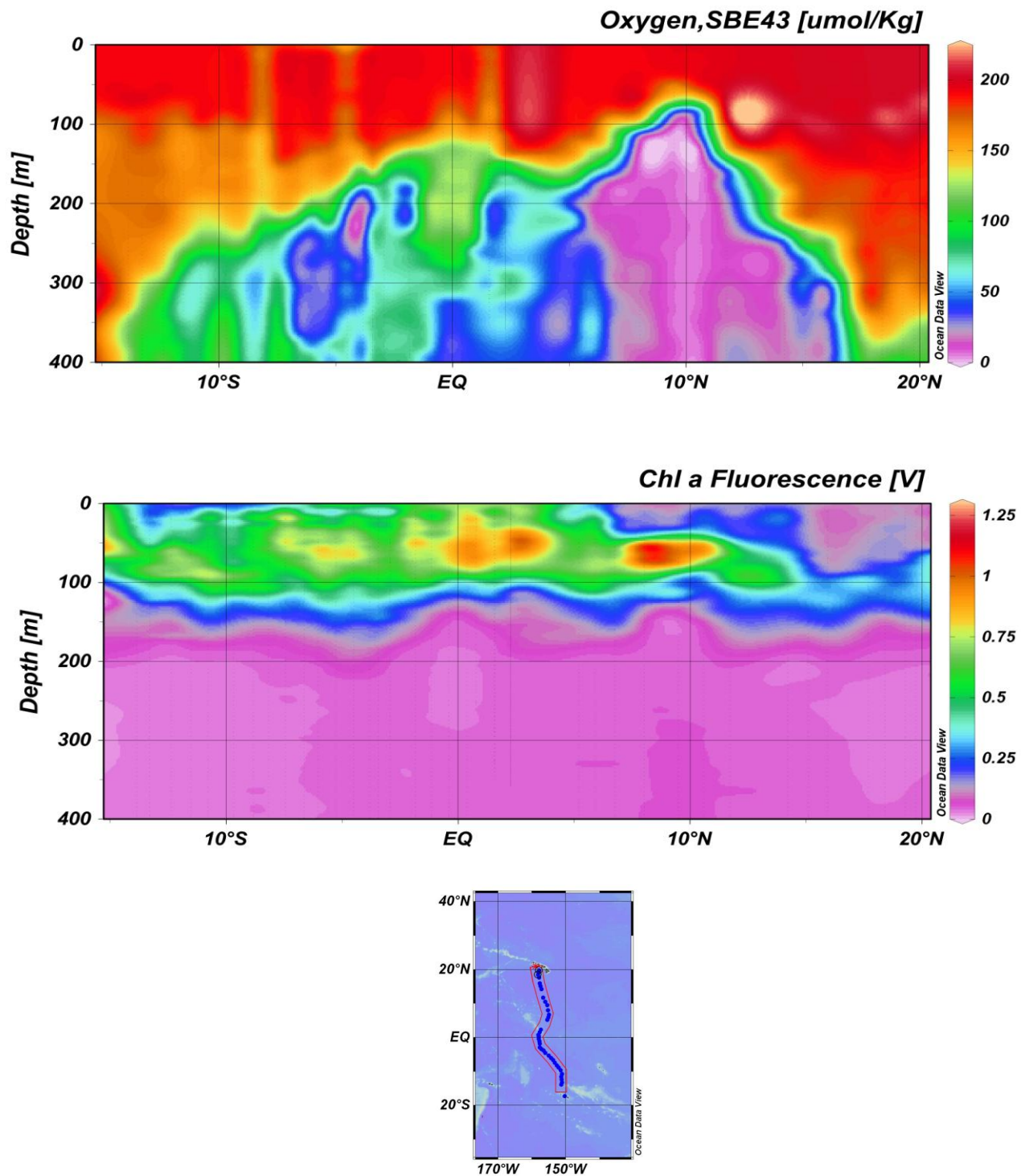


Figure 6. Oxygen (top) and raw fluorescence (middle) cross sections. The oxygen and fluorescence sensors are mounted on the carousel during hydrocast/CTD deployments. Blue dots on map (bottom) indicate locations of stations included in the section.

Table 4. S-244 Hydrocast (HC) bottle data. Blanks indicate no sample collected.

Station	Bottle #	Depth (m)	PO ₄ (μM)	NO ₃ (μM)	Chl a (ug/l)	pH	O ₂ Winkle (ml/L)
S244-002-HC	8	68.7				7.938	
S244-002-HC	13	0.0	0.11		0.186		
S244-003-HC	2	199.0	0.36	10.14	0.015		
S244-003-HC	3	99.2	0.10	1.52	0.219		
S244-003-HC	5	68.1				8.012	
S244-003-HC	6	49.3	2.08	0.36	0.171		
S244-003-HC	10	18.6	0.10	0.40	0.149		
S244-003-HC	12	9.8				8.058	
S244-003-HC	13	0.0	0.23	0.17	0.153		
S244-004-HC	13	0.0	0.01		0.230		
S244-005-HC	2	397.5				7.519	
S244-005-HC	3	297.9	0.90	31.83		7.695	
S244-005-HC	4	199.5			0.015	7.905	
S244-005-HC	5	118.8	0.32	2.11	0.188	7.940	
S244-005-HC	6	100.3			0.350		
S244-005-HC	7	85.3	0.08	0.34	0.263		
S244-005-HC	8	69.3				8.017	
S244-005-HC	10	30.1	0.08	0.41	0.135	8.013	
S244-005-HC	12	10.0				8.047	
S244-005-HC	13	0.0	0.07	0.25	0.155		
S244-007-HC	2	198.6	0.30	13.64	0.027		
S244-007-HC	3	99.6	0.08	0.16	0.346		
S244-007-HC	5	67.5				8.106	
S244-007-HC	6	49.4	0.11	0.16	0.124		
S244-007-HC	10	20.3	0.09	0.15	0.115		
S244-007-HC	11	10.8				8.131	
S244-007-HC	13	0.0	0.13	0.12	0.111		
S244-008-HC	1	497.0				7.266	
S244-008-HC	2	397.1	2.23			6.968	
S244-008-HC	3	296.4				7.314	
S244-008-HC	4	198.3	0.46		0.012	7.635	
S244-008-HC	7	69.8	0.10	0.26	0.214	7.924	
S244-008-HC	9	50.1	0.10		0.149		
S244-008-HC	10	20.0	0.12		0.101		
S244-008-HC	13	0.0	0.06	0.14	0.128		
S244-009-HC	2	198.2			0.009		
S244-009-HC	3	99.7	0.19	0.30	0.286		
S244-009-HC	5	67.0				8.018	
S244-009-HC	6	49.3	0.17	0.24	0.154		
S244-009-HC	9	19.8		0.19	0.139		
S244-009-HC	10	18.6	0.11				
S244-009-HC	11	10.6				7.908	
S244-009-HC	13	0.0	0.18	0.17	0.122		
S244-010-HC	13	0.0	0.13	0.05	0.158		
S244-011-HC	13	0.0	0.04		0.109		
S244-012-HC	1	480.3				6.059	

Table 4, continued.

Station	Bottle #	Depth (m)	PO ₄ (μM)	NO ₃ (μM)	Chl a (ug/l)	pH	O ₂ Winkle (ml/L)
S244-012-HC	3	297.7	2.00			6.884	
S244-012-HC	4	198.3			0.028		
S244-012-HC	5	148.5				7.169	
S244-012-HC	6	98.5	0.23		0.313		
S244-012-HC	7	69.4				7.791	
S244-012-HC	9	49.7	0.17		0.194	7.851	
S244-012-HC	11	10.6				7.858	
S244-012-HC	13	0.0	0.11		0.136		
S244-013-HC	2	397.3				7.328	
S244-013-HC	3	297.4	2.06	51.90	0.011	7.388	
S244-013-HC	5	99.5	1.60	37.93	0.149	7.478	
S244-013-HC	7	69.5				7.732	
S244-013-HC	8	49.6	0.21	1.03	0.372		
S244-013-HC	11	19.4	0.14	0.22	0.111	7.655	
S244-013-HC	13	0.0	0.12	0.09	0.099		
S244-014-HC	2	397.8	2.36			7.385	
S244-014-HC	3	298.8	2.15			7.398	
S244-014-HC	4	199.0			0.017		
S244-014-HC	5	149.0			0.150	7.838	
S244-014-HC	6	99.3	1.93	32.90	0.165		
S244-014-HC	7	69.8			0.352	7.792	
S244-014-HC	9	49.7	0.55	8.37	0.353	7.909	
S244-014-HC	11	9.9				8.080	
S244-014-HC	13	0.0	0.12		0.117		
S244-015-HC	2	398.7	1.89	68.50		7.421	
S244-015-HC	3	298.7	1.77	78.17		7.423	
S244-015-HC	4	199.6			0.013	7.415	
S244-015-HC	5	149.4			0.085		
S244-015-HC	6	99.3	0.54	22.21	0.292	7.677	
S244-015-HC	8	49.9	0.05	0.47	0.316		
S244-015-HC	10	19.6	0.03	0.24		8.044	
S244-015-HC	13	0.0	0.12	0.33	0.094		
S244-016-HC	2	478.3	2.19				
S244-016-HC	3	396.7				7.424	
S244-016-HC	4	298.0			0.010		
S244-016-HC	5	199.1	2.09		0.017	7.475	
S244-016-HC	7	129.2	0.88		0.185	7.733	
S244-016-HC	8	100.0			0.288		
S244-016-HC	9	69.1	0.06		0.335	8.021	
S244-016-HC	11	30.3	0.05		0.148		
S244-016-HC	13	0.0	0.12	0.19	0.117		
S244-017-HC	2	474.1	2.22	70.51		7.420	
S244-017-HC	4	297.5	1.85	66.46		7.456	
S244-017-HC	5	199.0			0.014		
S244-017-HC	6	149.3	0.79	18.11	0.103	7.696	
S244-017-HC	8	98.5			0.294		
S244-017-HC	9	69.6	0.12	1.99	0.286	8.011	

Table 4, continued.

Station	Bottle #	Depth (m)	PO ₄ (μM)	NO ₃ (μM)	Chl a (ug/l)	pH	O ₂ Winkle (ml/L)
S244-017-HC	11	30.0	0.16	0.93	0.246	8.057	
S244-017-HC	12	10.3				8.029	
S244-017-HC	13	0.0	0.20	0.52	0.171		
S244-018-HC	2	582.1	1.89			7.516	
S244-018-HC	4	397.9	2.22			7.552	
S244-018-HC	5	298.9			0.010		
S244-018-HC	6	198.3	1.60		0.012	7.541	
S244-018-HC	8	98.7	0.21		0.297	8.149	
S244-018-HC	9	70.0			0.325		
S244-018-HC	10	49.6	0.18		0.239	8.182	
S244-018-HC	11	25.4			0.272		
S244-018-HC	12	9.5				8.306	
S244-018-HC	13	0.0	0.15	0.91	0.235		
S244-019-HC	13	0.0	1.26	3.03	0.155		
S244-020-HC	1	348.5	1.97	38.10			
S244-020-HC	3	345.5				7.536	
S244-020-HC	5	199.3	1.57	47.43	0.017	7.569	
S244-020-HC	6	149.6			0.049		
S244-020-HC	7	124.4				7.540	
S244-020-HC	8	99.7	0.62	7.92	0.123	8.046	
S244-020-HC	10	50.1	0.66	7.50	0.258		
S244-020-HC	11	24.7			0.165		
S244-020-HC	12	10.4				8.046	
S244-020-HC	13	0.0	0.72	7.12	0.178		
S244-021-HC	1	289.9				7.522	
S244-021-HC	3	288.7	2.62			7.560	
S244-021-HC	4	199.0			0.006		
S244-021-HC	5	149.2			0.071		
S244-021-HC	6	99.6	0.89		0.149	7.910	
S244-021-HC	7	74.7			0.192		
S244-021-HC	8	49.5	0.51		0.261	7.997	
S244-021-HC	11	19.4	0.39		0.168	8.010	
S244-021-HC	13	0.0	0.52		0.082		
S244-022-HC	1	328.6	1.81			7.694	
S244-022-HC	4	298.5	3.04			7.526	
S244-022-HC	6	149.7	1.32		0.076	7.825	
S244-022-HC	8	100.5			0.214		
S244-022-HC	9	75.0	0.77		0.211	7.973	
S244-022-HC	10	49.9			0.210		
S244-022-HC	11	30.2			0.205	7.678	
S244-022-HC	13	0.0				8.005	
S244-023-HC	1	253.4	1.32	28.29		7.646	
S244-023-HC	4	199.5	1.12	34.43	0.010		
S244-023-HC	5	149.9			0.027		
S244-023-HC	6	99.2	0.92	11.53	0.257	7.976	
S244-023-HC	7	84.9			0.333		
S244-023-HC	8	50.3	0.72	10.17	0.299	8.014	

Table 4, continued.

Station	Bottle #	Depth (m)	PO ₄ (μM)	NO ₃ (μM)	Chl a (ug/l)	pH	O ₂ Winkle (ml/L)
S244-023-HC	11	18.8	0.57	9.45	0.227	8.014	
S244-023-HC	13	0.0	0.57	9.75	0.207		
S244-025-HC	1	402.9	0.98	18.94		7.924	
S244-025-HC	4	199.3	1.46	52.66	0.006	7.738	
S244-025-HC	5	150.0			0.022		
S244-025-HC	6	99.6	0.69	10.57	0.276	7.957	
S244-025-HC	7	75.3			0.395		
S244-025-HC	8	49.4	0.72		0.243	8.006	
S244-025-HC	11	19.0	0.82	11.45	0.219	7.995	
S244-025-HC	13	0.0	0.77	11.28	0.193		
S244-026-HC	1	454.7	1.40			7.782	
S244-026-HC	4	298.2	1.44			7.579	
S244-026-HC	6	149.5	1.20		0.081	7.842	
S244-026-HC	8	70.6			0.269		
S244-026-HC	9	37.7	0.52		0.290	8.006	
S244-026-HC	10	18.1			0.321		
S244-026-HC	11	18.0			0.317	8.024	
S244-026-HC	13	0.0	0.56	12.06	0.348	8.042	
S244-027-HC	2	397.0	2.34			7.549	
S244-027-HC	4	199.5	2.28	58.01	0.009	7.550	
S244-027-HC	6	99.5	0.49	6.62	0.281	7.964	
S244-027-HC	8	50.4	0.48	9.19	0.314	8.007	
S244-027-HC	11	19.7	0.38	10.95	0.252	8.003	
S244-027-HC	13	0.0	0.44	13.97	0.216		
S244-028-HC	2	496.3	2.00			7.440	
S244-028-HC	4	298.2	1.89			7.556	
S244-028-HC	6	149.9	0.94		0.121	7.856	
S244-028-HC	8	99.6			0.234	8.000	
S244-028-HC	9	74.5			0.251		
S244-028-HC	10	49.5	0.65		0.236	8.011	
S244-028-HC	11	29.8			0.221		
S244-028-HC	13	0.0	0.58	13.69	0.202	8.029	
S244-029-HC	1	458.2		180.95			
S244-029-HC	2	397.7	1.78			7.571	
S244-029-HC	4	198.1	1.58	42.80		7.566	
S244-029-HC	6	100.1	0.80	9.62	0.189	8.041	
S244-029-HC	7	74.7			0.211		
S244-029-HC	8	49.6	0.44		0.165	8.066	
S244-029-HC	11	18.8	0.52	7.53	0.143	8.037	
S244-029-HC	13	0.0	0.65	11.30	0.119		
S244-030-HC	2	480.5	2.01			7.286	
S244-030-HC	4	298.4	1.58			7.490	
S244-030-HC	6	149.5	1.01		0.138	7.853	
S244-030-HC	8	99.9	0.63		0.199	8.033	
S244-030-HC	9	74.0			0.234		
S244-030-HC	10	55.0	0.74		0.234	8.038	
S244-030-HC	11	29.9			0.205		

Table 4, continued.

Station	Bottle #	Depth (m)	PO ₄ (μM)	NO ₃ (μM)	Chl a (ug/l)	pH	O ₂ Winkle (ml/L)
S244-030-HC	13	0.0	0.54	11.25	0.192	8.047	
S244-031-HC	13	0.0	0.40	9.60	0.140		
S244-032-HC	2	496.1	2.09	54.38		7.511	
S244-032-HC	3	398.0	2.12				
S244-032-HC	4	298.0				7.436	
S244-032-HC	5	198.5	1.08	26.98			
S244-032-HC	6	148.9			0.168	7.898	
S244-032-HC	8	100.0	0.67	9.28	0.237	7.984	
S244-032-HC	9	75.2			0.302		
S244-032-HC	10	49.3	0.60		0.276	8.006	
S244-032-HC	11	25.0			0.219		
S244-032-HC	13	0.0	0.61	9.60	0.282	7.990	
S244-033-HC	13	0.0	0.52	9.71			
S244-034-HC	1	564.5	2.47			7.195	2.29
S244-034-HC	3	397.6	1.94			7.598	2.54
S244-034-HC	5	199.2	1.17			7.844	3.88
S244-034-HC	6	149.1			0.156		
S244-034-HC	8	99.4	0.70		0.162	8.066	4.88
S244-034-HC	9	69.1			0.285		
S244-034-HC	10	50.2	0.53		0.260	8.148	4.86
S244-034-HC	11	24.9			0.175		
S244-034-HC	12	10.5					4.94
S244-034-HC	13	0.0	0.48	8.48	0.187	8.240	
S244-035-HC	1	593.8	1.86	59.69		7.287	
S244-035-HC	4	199.2	0.76	17.13	0.014	7.837	
S244-035-HC	5	148.7			0.114		
S244-035-HC	7	80.1	0.51	8.04	0.198	7.978	
S244-035-HC	9	49.4			0.288	7.999	
S244-035-HC	10	20.1	0.44	7.85			
S244-035-HC	11	19.2			0.211	7.978	
S244-035-HC	13	0.0	0.12	5.32			
S244-036-HC	1	561.6	0.09				
S244-036-HC	4	298.2	0.10				
S244-036-HC	6	149.7	0.03		0.042		
S244-036-HC	8	99.5			0.258		
S244-036-HC	9	74.8			0.230		
S244-036-HC	10	49.9	0.08	6.64	0.224		
S244-036-HC	11	25.0			0.221		
S244-036-HC	13	0.0	0.14	7.96			
S244-037-HC	1	529.4	0.04			7.532	
S244-037-HC	3	297.6	0.16			7.579	
S244-037-HC	5	148.8	0.08			7.995	
S244-037-HC	6	124.5			0.230		
S244-037-HC	7	89.5	0.19	4.26	0.195	8.056	
S244-037-HC	8	50.0	0.15		0.201	8.058	
S244-037-HC	11	18.1			0.207		
S244-037-HC	13	0.0	0.41	6.37	0.157	8.070	
S244-038-HC	1	503.8	0.62			7.487	3.38

Table 4, continued.

Station	Bottle #	Depth (m)	PO ₄ (μM)	NO ₃ (μM)	Chl a (ug/l)	pH	O ₂ Winkle (ml/L)
S244-038-HC	4	297.8	0.18			7.580	3.37
S244-038-HC	5	199.3	0.16		0.012	7.874	4.21
S244-038-HC	8	98.6			0.321		4.60
S244-038-HC	9	74.8			0.251		
S244-038-HC	10	50.3	0.17		0.217	8.043	4.80
S244-038-HC	13	0.0	0.12	3.56	0.214		
S244-039-HC	1	459.0	0.15	58.71		7.407	
S244-039-HC	3	298.4	0.11			7.555	
S244-039-HC	5	148.3	0.28	8.50		7.995	
S244-039-HC	6	124.5			0.156		
S244-039-HC	7	89.5	0.13	1.86	0.294	8.058	
S244-039-HC	8	49.2	0.01		0.202	8.013	
S244-039-HC	11	19.0		1.60	0.145		
S244-039-HC	13	0.0		1.92	0.168	8.013	
S244-040-HC	1	595.7	0.20			7.460	2.63
S244-040-HC	4	298.2	0.16			7.584	
S244-040-HC	5	198.5			0.012	7.918	
S244-040-HC	7	122.5			0.157		
S244-040-HC	8	98.0	0.18		0.311	8.007	4.30
S244-040-HC	9	74.5			0.339		
S244-040-HC	10	48.6			0.278	8.118	5.44
S244-040-HC	13	0.0	0.11		0.248	8.084	
S244-041-HC	1	503.3	0.12	86.62			
S244-041-HC	3	267.7	0.08				
S244-041-HC	6	92.1	0.07		0.166		
S244-041-HC	7	66.1	0.21	3.65	0.231		
S244-041-HC	8	18.6	0.13		0.287		
S244-041-HC	11	18.4		2.07	0.129		
S244-041-HC	13	0.0	0.18	1.13	0.137		
S244-042-HC	1	568.3	0.19			7.483	
S244-042-HC	4	298.4	1.05			7.658	
S244-042-HC	5	198.5			0.013	7.902	
S244-042-HC	7	123.1			0.257		
S244-042-HC	8	98.4			0.327	8.019	
S244-042-HC	9	73.9	0.38		0.321		
S244-042-HC	10	50.5			0.156	8.082	
S244-042-HC	13	0.0	0.40	0.65	0.149	8.089	
S244-043-HC	1	584.9				7.545	
S244-043-HC	3	298.7				7.901	
S244-043-HC	4	198.3				7.936	
S244-043-HC	6	124.9			0.121		
S244-043-HC	7	88.1	0.56	3.43	0.300	8.052	
S244-043-HC	8	48.7			0.210		
S244-043-HC	11	18.8		0.64	0.151	8.239	
S244-043-HC	13	0.0	0.50	0.74	0.127		

Table 5. S-244 Neuston Net Tow (NT) data.

Station	Tow Distance (m)	Zoo. Density (ml/m ²)	Phyllo-soma (#)	Lepto-cephali (#)	Mycto-phids (#)	Cepha-lopods (#)	Other Nekton >2cm (#)	Total Nekton (#)	Total Nekton (ml)	Plastic Pellets (#)	Plastic Pieces (#)	Tar Pieces (#)	Halo-bates (#)	Gelatinous Organisms >2cm (#)	Gelatinous Organisms >2cm (ml)
S244-001-NT	2509.0	0.0068	1	1	9	4	9	24	12.0	0	1	0	69	16	6.0
S244-003-NT	1468.4	0.0122	1	0	1	0	4	6	5.5	0	6	0	100	5	5.5
S244-007-NT	1380.6	0.0065	0	0	0	0	1	1	<1	0	0	0	22	8	3.0
S244-009-NT	1856.5	0.0019	0	0	1	0	0	1	0.2	0	9	0	18	4	3.9
S244-011-NT	1811.0	0.0050	0	0	1	0	0	1	0.5	0	0	0	26	6	2.5
S244-013-NT	1543.7	0.0052	0	0	0	0	0	0	0.0	0	7	0	4	10	2.0
S244-015-NT	1795.0	0.0017	0	0	1	0	0	1	<1	0	6	0	3	1	<1
S244-017-NT	1295.5	0.1073	0	0	0	0	0	0	0.0	0	2	0	3	0	0.0
S244-019-NT	1932.9	0.0119	0	0	2	0	1	3	2.5	0	1	0	2	17	4.0
S244-020-NT	2574.9	0.0089	0	0	1	0	0	1	0.3	0	0	0	1	17	n/d ¹
S244-021-NT	1719.4	0.0268	0	0	11	0	0	11	1.4	0	0	0	0	58	7.0
S244-022-NT	3463.8	0.0015	0	0	0	0	0	0	0.0	0	0	0	0	0	0.0
S244-023-NT	2169.6	0.0097	0	0	19	0	2	21	4.0	0	0	0	0	13	17.0
S244-024-NT	2217.3	0.0090	0	0	0	0	0	0	0.0	0	3	0	0	3	5.0
S244-025-NT	2561.2	0.0172	0	0	97	0	4	101	n/d ¹	1	0	0	1	0 ²	0.0 ²
S244-026-NT	3034.9	0.0125	0	0	0	0	0	0	0.0	0	2	0	0	1	<1
S244-027-NT	2825.4	0.0428	0	0	5	0	3	8	4.5	0	0	0	1	1052	~2000
S244-028-NT	2640.2	0.0709	0	0	0	0	19	19	2.6	0	0	0	0	0	0.0

¹ n/d = not determined.

² S244-025-NT also contained 55 salps, each <2cm, so these are not included in the 'Gelatinous Organisms >2cm' columns.

Table 5, continued.

Station	Tow Distance (m)	Zoo. Density (ml/m ²)	Phyllosoma (#)	Leptocephali (#)	Myctophids (#)	Cephalopods (#)	Other Nekton >2cm (#)	Total Nekton (#)	Total Nekton (ml)	Plastic Pellets (#)	Plastic Pieces (#)	Tar Pieces (#)	Halobates (#)	Gelatinous Organisms >2cm (#)	Gelatinous Organisms >2cm (ml)
S244-029-NT	2807.0	0.0645	0	0	26	0	3	29	10.0	0	0	0	13	48 ³	16.0 ³
S244-030-NT	2367.3	0.0042	0	0	0	0	0	0	0.0	0	0	0	2	0	0.0
S244-031-NT	1914.3	0.0293	0	0	8	0	2	10	2.5	0	0	0	1	80	n/d ¹
S244-032-NT	1898.1	0.0063	0	0	0	0	2	2	0.1	0	0	0	0	1	0.1
S244-033-NT	1947.2	0.0662	0	0	5	0	1	6	2.0	0	0	0	0	55	5.5
S244-034-NT	1819.2	0.0027	0	0	0	0	1	1	2.0	0	1	0	2	1	1.0
S244-035-NT	1651.3	0.0103	0	0	11	0	0	11	3.0	0	3	0	5	7	2.0
S244-036-NT	1725.4	0.0017	0	0	0	0	0	0	0.0	0	3	0	0	0	0.0
S244-037-NT	1515.2	0.0310	0	0	0	0	1	1	1.0	0	1	0	1	4	0.5
S244-038-NT	1931.9	0.0585	0	0	0	0	3	3	2.0	1	0	0	1	0	0.0
S244-039-NT	2027.5	0.0242	0	0	0	0	2	2	0.4	0	0	0	2	21	2.3
S244-040-NT	2432.7	0.0021	0	0	0	0	0	0	0.0	0	0	0	5	0	0.0
S244-041-NT	2002.4	0.0310	0	0	11	0	0	11	n/d ¹	0	0	0	47	0 ⁴	0.0 ⁴
S244-042-NT	1919.4	0.0026	0	0	0	0	0	0	0.0	0	9	0	14	0	0.0
S244-043-NT	1589.0	n/d ¹	0	0	25	0	1	26	5.5	0	1	0	0	125	n/d ¹
S244-044-NT	3988.3	0.0023	0	0	39	0	1	40	5.5	0	3	0	2	0	0.0

¹ n/d = not determined.

³ S244-029-NT also contained 387 salps, each <2cm, so these are not included in 'Gelatinous Organisms >2cm' columns.

⁴ S244-041-NT also contained 59 salps, each <2cm, so these are not included in 'Gelatinous Organisms >2cm' columns.

Table 6. S-244 Meter Net Tow (MN) data. Each station was a paired net array, with Net A being deeper than Net B.

Station	Tow depth (m) ¹	Tow Volume (m ³)	Zoo. Density (ml/m ³)	Phyllo-soma (#)	Lepto-cephali (#)	Mycto-phids (#)	Cepha-lopods (#)	Other Nekton >2cm (#)	Total Nekton (#)	Total Nekton (ml)	Plastic pellets (#)	Plastic pieces (#)	Tar Pieces (#)	Halo-bates (#)	Gelatinous Organisms >2cm (#)	Gelatinous Organisms >2cm (ml)
S244-010-MN-A	~250	2236	0.017	0	0	0	0	0	0	0	0	49	0	0	0	0
S244-010-MN-B	~50	1246	0.028	0	0	0	0	0	0	0	0	26	0	0	0	0
S244-011-MN-A	~150	1949	0.034	0	0	3	0	4	7	3	0	0	0	0	11	7.5
S244-011-MN-B	~50	1032	0.062	0	0	0	0	0	0	0	0	0	0	0	19	n/d ²
S244-016-MN-A	142	2041	0.022	0	1	0	11	0	12	<1	0	11	0	0	0	0
S244-016-MN-B	~30	856	0.010	0	0	0	0	3	3	0.8	0	33	0	0	0	0
S244-017-MN-A	~250	2404	0.082	0	0	0	0	0	0	0	0	1	0	0	0	0
S244-017-MN-B	~50	918	0.172	0	0	0	0	0	0	0	0	3	0	0	0	0
S244-026-MN-A	132	4007	0.035	0	0	0	1	1	2	2	0	33	0	0	7	2.9
S244-026-MN-B	~50	3217	0.036	0	0	0	0	2	2	0.8	0	293	0	0	34	2.5
S244-027-MN-A	~200	4025	0.050	0	0	32	1	42	75	26.5	0	0	0	0	3	5.0
S244-027-MN-B	~50	1265	0.097	0	0	3	0	13	16	2.5	0	0	0	0	25	28.0
S244-032-MN-A	~250	2292	0.027	0	0	0	0	0	0	0	0	139	0	0	41	6.5
S244-032-MN-B	~50	1572	0.036	0	0	0	0	0	0	0	0	7	0	0	237	n/d ²
S244-033-MN-A	~250	3490	0.036	0	0	25	0	35	60	13.3	0	43	0	0	15	7.0
S244-033-MN-B	~50	1687	0.113	0	0	0	0	2	2	0.2	0	0	0	0	29	14.1
S244-036-MN-A	~250	3919	0.023	0	0	0	0	2	2	0.5	0	3	0	0	52	27.5
S244-036-MN-B	~50	1608	0.075	0	0	0	0	0	0	0	0	3	0	0	119	56.0
S244-037-MN-A	~250	3497	0.038	0	1	26	0	29	56	7.5	0	0	0	0	65	19.0
S244-037-MN-B	~50	997	0.093	0	1	0	0	0	1	0.5	0	0	0	0	76	15.5

¹ Most tow depths approximated based on wire angle; ² n/d = not determined.

Table 7. S-244 Tucker Trawl (TT) data.

Station	Net #	Tow Depth Range (m)	Tow Volume (m ³)	Zoo. Density (ml/m ³)	Phyllo-soma (#)	Lepto-cephali (#)	Mycto-phids (#)	Cepha-lopods (#)	Other Nekton >2cm (#)	Total Nekton (#)	Total Nekton (ml)	Plastic Pellets (#)	Plastic Pieces (#)	Tar Pieces (#)	Halo-bates (#)	Gelatinous Organisms >2cm (#)	Gelatinous Organisms >2cm (ml)
S244-005-TT	1&3	0-100	1549.2	0.046	1	0	3	0	7	11	4.0	0	31	0	0	10	n/d ²
S244-005-TT	2	100-200	2251.7	0.015	0	11	1	0	3	15	5.0	0	6	0	0	1	1.0
S244-006-TT	1	0-65	1365.1	0.017	0	0	0	0	0	0	0.0	0	9	0	0	0	0.0
S244-006-TT	2	65-155	2510.1	0.018	0	0	0	0	0	0	0.0	0	9	0	0	1	2.0
S244-006-TT	3	0-65	dnc ¹	dnc ¹	-	-	-	-	-	-	-	-	-	-	-	-	-

¹ dnc = Net #3 of Tucker Trawl S244-006-TT did not close. No useable sample recovered; ² n/d = not determined.

STUDENT RESEARCH ABSTRACTS -

Are Barrier Layers Indicative of Imminent ENSO Events?

Michela Cupo and Shenandoah Raycroft

Barrier layers (BLs) occur when the pycnocline is shallower than the thermocline because of salinity stratification. The phenomenon affects physical and biological cycles within the ocean as BLs limit vertical mixing. Previous studies have suggested that BL distribution and abundance are linked to El Niño Southern Oscillation (ENSO); however, the nature of this relationship is relatively unknown. We hypothesized that an increase in BL abundance would characterize the shift into an El Niño event and, conversely, that a decrease in BL abundance would characterize the shift into La Niña events. The *SSV Robert C. Seamans* sailed from Honolulu, Hawaii to Papeete, Tahiti from mid-November through December 2012, during a neutral period in the ENSO cycle. Along our cruise track, 35 stations were sampled with a CTD. The data were analyzed for the presence and thickness of barrier layers by calculating and then comparing the pycnocline and thermocline depths. Seven stations contained BLs, ranging in thickness from 15 to 60 meters. Their distribution did not correlate with any particular oceanographic region. Data from four previous SEA cruises, each that sailed during a different stage of an ENSO cycle, were also examined for barrier layers. In order to compare years of data with different numbers of samples, the data (number of stations yielding BLs) were standardized as a percent of the total number of stations. These data were then analyzed in relation to the Southern Oscillation Index (SOI) to provide a context for ENSO cycling. Although our hypothesis was not specifically supported, the data suggest that barrier layer abundance may be negatively correlated with increasing SOI. This would mean that a greater abundance of barrier layers may characterize El Niño events in the central/eastern tropical Pacific, which is perhaps due to greater precipitation in the region during such time periods. This warrants continued study on future cruises, to further explore the possible relationship between barrier layers and ENSO cycles.

Pacific Salp Gut Chlorophyll Content vs. Salp Size, Environmental Chlorophyll-a Concentration, and Salp Density

Jack Fields

Salps are important pelagic grazers on plankton in coastal and open ocean environments worldwide. Individuals can grow extraordinarily fast, and the density of salps in a particular area can bloom and decrease quickly in response to change in plankton density. Salps are indiscriminate filter feeders, and they play an important role in the biological carbon pump because of their fast filtration rates and large fecal pellets. These pellets sink quickly, providing a significant transport pathway of carbon to the deep sea. Various researchers have attempted to quantify the magnitude of this process by looking at salp gut chlorophyll-a content, as a proxy for grazing rate. Salps were collected in neuston and meter nets during SEA Cruise S-244, a meridional transect of the central Pacific from Hawaii to Tahiti during the late fall of

2012. Salp distribution was found to be quite patchy and sporadic, with abundance counts in the tows ranging from 0 to 1042; tows containing the greatest numbers were collected south of the Equator. The length and biovolume of many of the individual salps were measured. The gut contents of selected salps were removed, and the chlorophyll-a pigment of the samples was extracted with acetone and analyzed using fluorometric techniques. Results suggest that chlorophyll-a content has a weak positive correlation with both salp length and salp biovolume, although this is based on a limited number of samples of non-optimal size distribution. It appears that larger salps may have more potential for transporting greater amounts of carbon to the deep sea, which is in agreement with the results of prior studies.

Effects of El Nino Southern Oscillation on the Equatorial Undercurrent Heat Transport

Souha Ouni

The Equatorial Undercurrent (EUC) is an eastward-flowing undercurrent centered on the equator in the Pacific Ocean. This undercurrent develops as a result of surface currents pushing equatorial water westward, which causes a pool of water to accumulate on the western side of the ocean basin, which creates a pressure gradient that forces water from as deep as 150 m to flow east to regain a pressure balance. Although this undercurrent flow is always present, its velocity, width, and depth change seasonally and inter-annually. The westward surface currents are highly influenced by El Nino Southern Oscillation (ENSO) cycles, being stronger during La Nina events and weaker during El Nino events. These events influence the flow and transport of the EUC as well. This study measured the magnitude of the eastward EUC flow during the late fall of 2012 on SEA cruise S-244 (SOI ~ 2.4). By combining those data with temperature data from CTD stations collected during the cruise, a total eastward heat transport of 7.31 PW was calculated for the EUC. Similar heat transport calculations were made for SEA Cruise S-238 (1.62 PW, during an La Nina year with SOI ~ 23.0) and for SEA Cruise S-226 (2.54 PW, during a weak El Nino year, SOI ~ -7.0). These results were unexpected, in that stronger current flows during La Nina periods were projected to correlate with a relatively higher level of EUC heat transport. Reasons from these results are not clear, although water temperature profiles, which also vary with ENSO, play a role in the calculations. Due to the importance of heat transport in climate modeling, further research is warranted.

Measuring Skipjack Tuna Habitat in the Central Equatorial Pacific

Trevor Kauffman

Skipjack tuna are an important commercial species that are widely distributed in the Pacific Ocean. Stock assessments are difficult to make because of the vast distribution of the species, and most stock assessments are based on fisheries data. Because there are limited fisheries data for the central equatorial Pacific, the location of the SEA S-244 cruise track, another method of stock assessment would be useful.

In this study, an index is developed to evaluate the central equatorial Pacific in terms of its suitability as skipjack tuna habitat. The index is based on measured parameters known to be constraining to skipjack tuna: dissolved oxygen (DO), seawater temperature, and abundance of prey. Because it was outside of our means to measure prey directly, an indirect method using zooplankton diversity and density was used. The resulting index shows the habitat suitability varying significantly along our meridional transect from Hawaii to Tahiti, with some areas being limited by DO, some by temperature, and some by prey abundance. Measured from the ocean surface, the thickness of the water column suitable for skipjack habitation based on physical parameters (DO > 3.5 ml/L and water temperature > 18°C) ranged from 62 to 288 meters; temperature was the limiting parameter in the subtropical gyres and DO was the limiting parameter in the equatorial region. When combined with prey abundance data, the overall 'Skipjack Habitat Index' values suggest that the central equatorial region south of the Equator may be slightly more suitable for skipjack habitat than regions north of the equator, which is consistent with distribution data of skipjack tuna catch by commercial fisheries. However, this is not definitive, and further research along the lines of this study and more extensive skipjack catch data would be needed to verify this observation. Additional studies are also warranted to explore the interactions between ENSO, global warming, seasonal climate shifts, and tuna habitat.

Cyanobacteria Abundances Along an Equatorial Pacific Cruise Track

Ariel Christensen and Samantha Allen

Bacteria are an important part of the microbial loop, which contributes significantly to the oceanic biological pump. *Prochlorococcus* and *Synechococcus* are the two most abundant types of cyanobacteria in the oceans, thriving in differing environments. This study explored the distribution of both types of cyanobacteria along the cruise track of SEA Cruise S-244, a meridional transect of the central equatorial region from Hawaii to Tahiti. Twelve water samples were collected from 6 stations in different oceanographic regions, one sample from near the surface and one sample from the 1% light level at each station. Bacteria in these samples were counted using an epifluorescence microscope, and these data were compared with environmental parameters measured at the same locations. Total bacteria counts ranged from a minimum of 4,632/ml to a maximum of 24,676/ml, with *Synechococcus* being more abundant than *Prochlorococcus* in all samples. *Synechococcus:Prochlorococcus* ratios ranged from 1.8:1 to 79.6:1, with generally higher ratios south of the equator. Contrary to what we expected, no correlations were observed between cyanobacteria abundance and the environmental parameters of dissolved oxygen content, nitrate, or phosphate. This may be due, at least in part, to the relatively small variation in these parameters observed along our cruise track. *Synechococcus* abundance shows a weak positive correlation with water temperature ($R^2=0.65$).

Dimethylsulfoniopropionate (DMSP) Potential Production in the Equatorial Pacific Biogeochemical Sulfur Cycle: A Measure of Phytoplankton Abundances

Darcy Balcarce and Simona Clausnitzer

Marine dimethylsulfide (DMS) is a major source of atmospheric sulfur, accounting for 50% of the biogeochemical sulfur cycle and affecting the albedo of the clouds regionally, thus having influential effects on global heat regulation in a changing climate. Dimethylsulfoniopropionate (DMSP) is a precursor to DMS, which is produced in different amounts by various species of phytoplankton. The El Niño Southern Oscillation (ENSO) is a major inter-annual Pacific climate cycle that has been shown to dramatically affect water temperature and nutrient availability, and hence phytoplankton growth. This, in turn, likely influences DMSP concentrations and DMS production. This study measured relative abundances of dinoflagellates and diatoms at 15 stations during SEA Cruise S-244, a meridional transect from Hawaii to Tahiti conducted during the fall of 2012, at a neutral/transitional stage in the ENSO cycle. Relative abundance data were determined by 100 counts of organisms found in samples from the mixed layer. We found consistently higher abundances of diatoms than dinoflagellates at all stations, averaging 79.5% and 20.5%, respectively. A proxy measurement of the DMSP potential production of these organisms was calculated by multiplying the relative abundance data by DMSP potential production values available from the published literature (38 ± 18 mM for diatoms; 640 mM for dinoflagellates). This was then compared with data collected in 2011 during SEA Cruise S-238, a similar transect conducted during a La Niña event. Based solely on relative abundance data, the DMSP potential production for the stations occupied during 2012 averaged $16,883 \pm 5,548$ mM, which is not significantly different than that measured in the same region during the 2011 La Niña ($15,799 \pm 5,645$ mM). Information about the absolute abundances of both phytoplankton groups was not available, which argues for further research into this important scientific question in this relatively remote and unstudied part of the world.

Effects of Predator Presence, Biodiversity, and Nighttime Light Intensity on Diel Vertical Migration in the Equatorial Pacific

Ashley O'Neill and Brendan O'Flaherty

Diel vertical migration (DVM) is a common zooplankton migration pattern with important implications for the global carbon cycle. This study focused on how biodiversity, key predators, nighttime light levels, and primary productivity affect the magnitude of migrating biomass in the central equatorial Pacific. Zooplankton were sampled with surface neuston net and deeper oblique net tows during SEA Cruise S-244, a meridional cruise track that traversed several distinctive oceanographic regions between Hawaii and Tahiti in the late fall of 2012. Day/night tow pairs (10 neuston pairs and 6 pairs of deeper net tows) were collected in different oceanographic regions and at different moon phases. As expected, biodensities of the recovered zooplankton samples were almost always higher in the nighttime tows than during the paired daytime tows, indicating that DVM was observed. The magnitude of migrating biomass was determined by subtracting the daytime

biodensity from the night biodensity. In general, the magnitude of migrating biomass correlated negatively with biodensity, key predator counts (chaetognaths and myctophids), and chlorophyll-*a* (as a primary productivity proxy), and correlated positively with moon phase. These results are largely contrary to what we expected and, in some cases, also in conflict with previous laboratory and field studies. However, these correlations were all weak (maximum $R^2 < 0.5$), likely due to limitations in our design paradigm and the inherently complex influences on migrating biomass density. Additional study is required to further examine these relationships more definitively.

Phytoplankton Size and Total Primary Production in Four Distinct Oceanic Environments

Ivan Duong, Hayli Kinney, and Rebecca Lehman

It has been shown that picophytoplankton (0.2 to 2 μm) are responsible for the majority of primary production in low-nutrient oligotrophic oceanic environments. This paper details the contributions of different-sized phytoplankton to primary production along a cruise track from Honolulu, Hawaii (21°N, 158°W) to Papeete, Tahiti (17°S, 150°W). We sampled four oceanic zones, which we defined by latitude according to surface currents and thermocline depth at the time of sampling. We hypothesized that smaller phytoplankton would contribute more to primary production in the nutrient-poor North Pacific and South Pacific Subtropical Gyres (NPSG and SPSG), and that bigger phytoplankton would be the main contributors in the more nutrient-rich Equatorial Upwelling Zone (EUZ) and the South Equatorial Zone (SEZ). Water samples from the upper mixed layer at 16 stations were serially filtered and the chlorophyll-*a* content of three size fractions (0.3-3 μm , 3-8 μm , and >8 μm) were determined, providing a proxy for primary productivity of each fraction. The resulting size fraction percentages showed considerable variation. Smaller-sized phytoplankton were dominant in the NPSG samples and larger-sized phytoplankton were dominant in the EUZ and SEZ regions, as expected, although larger-sized phytoplankton were also most abundant in the SPSG samples. The chlorophyll-*a* content of the largest size fraction (>8 μm) had a weak positive correlation with both nitrate and phosphate abundance ($R^2 = 0.74$ and 0.44, respectively). This may reflect the fact that smaller phytoplankton, with greater surface area:volume ratios, have a competitive advantage in nutrient-poor environments. Water temperature may also have influenced the results, although it did not vary significantly along our cruise track and thus was not taken into account. We also measured the average size of individual dinoflagellates of the genus *Ceratium* along our cruise track. 13 phytoplankton net samples were examined for *Ceratium*, and the distance from the head of the central body to the base of the antapical horn was measured for 30 individuals from each sample. Again, the data displayed considerable variation, but it is interesting to note that the largest individuals (those >100 μm) were present only in the more nutrient-rich EUZ and SEZ regions. Further research, with improved methodology, is necessary to better demonstrate any correlations here.

Patterns of *Myctophid* Distribution and Diversity in the Central Pacific

Katie Blacketor

This study looked at the distribution and diversity of myctophids in the Central Pacific between Hawaii and Tahiti, as collected during SEA Cruise S-244 in the fall of 2012. Myctophids are a common mesopelagic fish that migrate to the surface of the ocean at night. The large abundance of myctophids worldwide allows for characterization of different zoogeographic regions. The purpose of this study was to establish trends between the distribution of species and the physical and biological parameters of the ocean. Along the cruise track, myctophids were collected in nighttime surface neuston and deeper net tows. A total of 353 myctophids were collected, 286 from the neuston tows and 67 from the deeper tows. The tow with the greatest number of myctophids ($n=97$) was collected in the equatorial region. Generally speaking, tows from near the equator and from south of the equator contained more myctophids than did tows from north of the equator. *Myctophum auro-lanturnatum* was the most abundant species, representing 87% of the myctophids that could be identified. Myctophid abundance was not correlated with chlorophyll-*a* content (as a proxy for primary productivity), surface water temperature, or salinity. The tow containing the greatest number of myctophids also had the greatest zooplankton density, suggesting a weak positive correlation between the two. The reasons for this correlation are unclear, and a previous SEA student found exactly the opposite trend.

Heat Transport Along a Meridional Transect of the Pacific Equatorial Region

Marta Trodahl and Jennifer Fardy

In order to better understand Earth's climate, it is vital to look at ocean heat transport and the systems that may affect it. In the tropical latitudes the ocean transports more heat than the atmosphere does. Equatorial oscillations like the El Niño Southern Oscillation (ENSO) and the Pacific Decadal Oscillation (PDO), which affect sea surface temperatures and wind patterns, may also have detectable effects on meridional ocean heat transport near the Pacific equator. Previous studies suggest that a large El Niño event and a corresponding PDO regime shift have led to intensified northern heat transport from 1998 to the present. We therefore hypothesized that if we were to calculate ocean heat transport from observational hydrographic data collected along a meridional transect of the central equatorial Pacific ($12^{\circ}\text{N} - 12^{\circ}\text{S}$) for three different post-1998 cruise tracks, that we would see more northern heat transport than southern. We found this to be true for SEA Cruise S-232 in November/December 2010, and for SEA Cruise S-238 in November/December 2011. However, for our cruise, S-244 in November/December 2012, we saw almost the completely opposite transport, with almost exclusively southward transport observed in both hemispheres. Total northern heat transport calculated from the northern stations was -1.8990 PW and from the southern stations was -0.0614 PW, with the negative values indicating southerly transport. Since this is merely one transect of the ocean during just one time of year, we cannot draw any conclusive results about the reverse in heat transport, but transport anomalies seem to be a precursor of SST anomalies and might therefore provide an earlier sign of

shifts in large-scale oscillations like ENSO and PDO. Additional studies of heat content and heat transport in the tropical Pacific Ocean are needed to further explore this possibility.

Pteropod Distribution in the Equatorial Pacific: Implications of Acidifying Waters

Mindy Alexander and Mary Rutz

With increasing levels of carbon dioxide in the world's atmosphere, ocean water chemistry is changing and affecting the various organisms that live within it. As the oceans act as a global carbon sink, carbon dioxide dissolves into seawater and the pH is lowered. This process, known as ocean acidification, hinders the ability of many organisms, such as pteropods, to produce shells that are formed of calcium carbonate. SEA Cruise S-244 sailed from Honolulu, Hawaii to Papeete, Tahiti, from November 15, 2012 to December 23, 2012. Surface neuston and deeper net tows were collected along the cruise track, and pteropod densities were calculated based on 100 counts of the recovered biomass in each tow. pH values were determined from water samples collected at the tow locations, and averaged over the depths at which the tows were taken. Resulting averaged pH values ranged from 7.5 to 8.1, with higher pH characteristic of shallower waters and an obvious shoaling of lower pH in an upwelling zone at about 10°N. We expected to find a positive correlation between pH and pteropod density, with regions of lower pH having lesser amounts of pteropods. Our results do not clearly show this relationship, but it is interesting to note that pteropod densities were consistently low ($<0.1 \text{ ml/m}^2$) in ocean waters with an average pH of less than about 7.8. Although numerous previous studies have focused on the effect of varying pH on different organisms in controlled laboratory settings, further studies are needed to further explore the effect of varying pH on organisms in a more complex field environment.

Going With the Flow: An Analysis of Surface Water Masses in the Equatorial Pacific

Madison Halloran and Leona Waller

The Pacific Ocean is a vast, diverse body of water. Its surface alone contains many different water masses, characterized by their movement, conservative properties, and biological inhabitants. This study analyzed hourly surface data collected on SEA Cruise S-244, a north to south transect of the central equatorial Pacific from Hawaii to Tahiti, in order to identify the surface water masses through which we passed. Based on surface temperature, salinity, chlorophyll-*a*, and current data, we identified eight discrete oceanographic regions: the North Pacific Subtropical Gyre, the Northern Equatorial Current, the North Equatorial Countercurrent, the Intertropical Convergence Zone, an Equatorial Upwelling zone, the South Equatorial Current, the South Equatorial Countercurrent, and the South Pacific Subtropical Gyre. The boundaries of many of these regions were shifted slightly north from what we had expected based on studies published by previous researchers. We also compared both the location and the oceanographic properties of the waters in each region to similar data from three previous SEA cruises that sailed during different El Niño

Southern Oscillation (ENSO) phases. We identified substantial differences in the data from these cruises, particularly in terms of temperature variations with latitude, likely relating to variations in the prevalence of equatorial upwelling in El Nino versus La Nina years. Based on these comparisons, we conclude that the late fall of 2012, during which S-244 sailed, displays remnants of the recent 2011 La Nina event as we move into a more neutral ENSO stage.